Reliability of the Freehand Region-of-Interest Method in Quantitative Cerebral Diffusion Tensor Imaging

Ullamari Hakulinen (ullamari.hakulinen@pshp.fi)
Department of Medical Physics, Medical Imaging Center of Pirkanmaa Hospital District, Tampere

Antti Brander
Department of Radiology, Medical Imaging Center of Pirkanmaa Hospital District, Tampere

Tero Ilvesmäki
Faculty of Medicine and Health Technology, Tampere University, Tampere

Mika Helminen
Tays Research Services, Tampere University Hospital, Tampere

Juha Öhman
Department of Neurosurgery, Tampere University Hospital and Tampere University, Tampere

Teemu Luoto
Department of Neurosurgery, Tampere University Hospital and Tampere University, Tampere

Hannu Eskola
Faculty of Medicine and Health Technology, Tampere University, Tampere

Research Article

Keywords: Diffusion tensor imaging, Reliability, Repeatability, Intra-class correlation coefficient, Fractional anisotropy, Apparent diffusion coefficient, Axial diffusivity, Radial diffusivity, ROI-based method, Freehand method.

Posted Date: February 8th, 2021

DOI: https://doi.org/10.21203/rs.3.rs-140421/v1

Abstract

Background: Diffusion tensor imaging (DTI) is a magnetic resonance imaging (MRI) technique used for evaluating changes in the white matter in brain parenchyma. The reliability of quantitative DTI analysis is influenced by several factors, such as the imaging protocol, pre-processing and post-processing methods, and selected diffusion parameters. Of the post-processing methods, the region-of-interest (ROI) method is most widely used because it is found in commercial programs. The focus of our research was to study the reliability of the freehand ROI method using various intra- and inter-observer analyses.

Methods: This study included 40 neurologically healthy participants who underwent diffusion MRI of the brain with a 3T scanner. The measurements were performed at nine different anatomical locations using a freehand ROI method. The data extracted from the ROIs included the regional mean values, intra- and inter-observer variability and reliability. The used DTI parameters were fractional anisotropy (FA), the apparent diffusion coefficient (ADC), and axial (AD) and radial (RD) diffusivity.

Results: The average ICC of the intra-observer was found to be 0.9 (excellent). The single ICC results were excellent (> 0.8) or adequate (> 0.69) in eight out of the nine regions in terms of FA and ADC. The most reliable results were found in the frontobasal regions. In terms of the regional mean values, significant differences between age groups were found in the frontobasal regions. Specifically, the FA and AD values were significantly higher and the RD values lower in the youngest age group (18-30 years) compared to the other age groups.

Conclusions: The quantitative freehand ROI method can be considered highly reliable for the average ICC and mostly adequate for the single ICC. The freehand method is suitable for research work with a well-experienced observer. Measurements should be performed at least twice in the same region to ensure that the results are sufficiently reliable. In our study, reliability was undermined by artifacts in some regions such as the cerebral peduncle, corona radiata and centrum semiovale. From a clinical point of view, the results are most reliable in adults under the age of 30, when age-related changes in brain white matter have not yet occurred.

Background

Diffusion tensor imaging (DTI) is a magnetic resonance imaging (MRI) technique that has become a popular tool for central nervous system imaging (1, 2). DTI is based on the diffusion characteristics of water molecules, which, in turn, reflect the histological structure of the tissue (3). Diffusion data can be used to calculate several quantitative parameters, such as fractional anisotropy (FA), the apparent diffusion coefficient (ADC), and axial (AD) and radial (RD) diffusivity. FA indicates the degree of diffusion anisotropy. The diffusion is generally strongest in the orientation parallel to the nerve tracts. The ADC expresses the mean diffusion in each direction. AD can be considered to be modulated by the axonal integrity (4, 5), and its changes can thus reflect the degree of axonal degeneration (6). RD, on the other hand, is modulated by axonal myelination (4, 5).

Several studies on different neurological diseases have utilized these DTI indices as biomarkers of the white matter integrity (7–11). Significant age-related changes in the integrity of white matter have also been found in healthy volunteers (12–17).

In chronic white matter diseases as well as in normal aging, FA values decrease while RD values increase (18–25). A strong relationship has also been found between the changes in axial diffusion and axonal injury (4). Moreover, ADC values may temporarily decrease in the acute phase of cerebrovascular accidents, but, in the chronic phase, they usually increase (26, 27).

The imaging process includes several steps between acquisition and the final parametric result calculated in the post-process results, and each step is susceptible to different pitfall sources (28–29). Specifically, low resolution, a low signal-to-noise ratio (SNR), and a variety of different types of artifacts can reduce the image quality (30–33). In particular, the single-shot echo-planar technique used in diffusion imaging can cause severe image distortions because of the long echo trains that are used in the sequence. The consequence of susceptibility artifact is geometric distortions at the interfaces between the soft tissue and air at the base of the skull in the head region (34). In addition, B_0 inhomogeneities cause a decrease in the efficiency of fat-saturation pulses (34). Protons in water and protons in fat tissue have different Larmor frequencies, which leads to fat-miss registration in single-shot echo-planar imaging. All of the above-mentioned pitfalls and artifacts also have a detrimental effect on the reliability of parametric results.

Post-processing and analysis methods can be selected according to whether individual or group results are required. The histogram (35), region-of-interest (ROI), and quantitative tractography methods (36) are suitable for both individual- and group-level analysis. In addition, the tract-based spatial statistics (TBSS) method (37) is an option for group analysis. Nowadays, different methods are often used concomitantly, giving additional value to the accuracy of the results (38–39).

The ROI method is still a highly valid method when measuring individual subjects. While laborious, time-consuming, and observer-dependent, it is still the most readily available method in commercial clinically approved software. The method can be used to evaluate the focal areas of brain parenchyma of a single subject and it enables leaving artifacts outside the area of measurement. The low or moderate repeatability of the method as well as its high intra- and inter-observer variation have been considered its cons (40).

The main objective was to investigate the reliability of the freehand ROI method, which includes intra- and inter-observer variation and repeatability measurements. The study examines how the number of measurements and artifacts affect the reliability of the results. A secondary objective was used to compare the repeatability between the different DTI parameters (FA, ADC, AD, and RD). In addition, the effects of age on changes in white matter are studied with group comparison. Correlation for FA and ADC parameters and age have already been published in our previous study using two ROI method (41). In this study, we also present the AD and RD result with a freehand ROI.

Methods

Subjects

Participants included 40 healthy adult volunteers consisting of 20 women and 20 men with an age range of 18–60 years and a mean age of 40.6 (SD 12.2) years (41, 42). The age groups were: (i) 18–30, (ii) 31–40, (iii) 41–50, and (iv) 51–60 years. Each age group included five men and five women. Thirty-nine of the subjects were right-handed, and one was left-handed. MRI scans were performed within a year (2010–2011). The criteria for assembling the control group were age and gender. The exclusion criteria consisted of the following: (i) neurological problems (including abnormalities upon neuroimaging), (ii) psychiatric problems, (iii) history of traumatic brain injury, (iv) former neurosurgical procedure, (v) problems with hearing or vision, (vi) first language other than Finnish, (vii) MRI contraindications, and (viii) refusal to participate. No indications of significant structural abnormalities were found in any of the subjects in conventional clinical sequences. An ethics approval was obtained from the Ethical Committee of the Pirkanmaa Hospital District, and written consent was obtained from each volunteer.

MRI Acquisition

The subjects were scanned with a 3T Siemens Trio (Siemens Healthcare, Erlangen, Germany) MRI scanner. The MRI protocol included sagittal T1-weighted 3D IR-prepared gradient echo, axial T2-weighted turbo spin echo, conventional axial and high-resolution sagittal fluid attenuation inversion recovery (FLAIR), axial T2*-weighted, and an axial susceptibility weighted imaging (SWI) series. The DTI data was collected by a single-shot, spin echo-based, and diffusion-weighted echo planar imaging sequence. The parameters for the DTI sequence were TR 5144 ms, TE 92 ms, FOV 230 mm, matrix 128 × 128, 3 averages, slice/gap 3.0/0.9 mm, voxel dimension 1.8 × 1.8 × 3.0 mm^3, b-factor 0, 1000 s/mm^2, and 20 diffusion gradient orientations. A 12-channel head coil and a four-channel neck coil were simultaneously used. The coils used in the study were subjected to regular quality tests throughout the study, so that they could be proven to be intact and of high quality.

Data Analysis

The multidirectional diffusion data was visually analyzed for distortions and artifacts. The eddy current distortion was qualitatively estimated by drawing the brain contours to the b_0 image and copying the contours to the diffusion weighted images. Susceptibility and phase artifacts were verified by reviewing the FA, ADC, AD, RD, and b_0 maps slice-by-slice.

The SNR was determined according the National Electrical Manufacturers Association (NEMA) standards 1-2008 with the expression SNR = S/N, where S = the signal and N = the noise of the image, which was estimated with a Rayleigh distribution (SD = standard deviation): N = SD/0.66. SNR values were measured from the b_0 images in each region (b = 0 s/mm^2).

Two experienced observers, a medical physicist (UH) and a neuroradiologist (AB), performed freehand measurements on a workstation using commercially available software Neuro3D (Siemens Healthcare, Malvern, USA). The freehand ROIs were manually placed on the axial images of the color-coded FA maps and automatically transferred to the ADC, AD, and RD maps as well as the non-diffusion weighted b_0 images. The ROIs were centered in the region using color-coded directions. The measurements were aimed to avoiding border areas, such as areas overlapping with cerebrospinal fluid spaces, partial volume effects, and neighboring tracts. The thalamus was drawn to the grayscale FA map, because the border areas were more clearly distinguishable than in the color map.

Slices containing artefacts were avoided. If this was not possible, the artefact areas were excluded by omitting them from the ROI regions (Fig. 1 and Fig. 2). The sizes of the ROIs were chosen using the anatomical knowledge of brain regions and a tract-based atlas of human white matter anatomy (43). The ROI size ranged from 10 mm^2 (min, cerebral peduncle) to 430 mm^2 (max, centrum semiovale). The time between the first and repeated freehand ROI measurements was at least four weeks.

Intra-observer measurements were performed for all volunteers (n = 40) and inter-observer measurements for 15 volunteers (n = 15). Nine regions were measured, eight of which were in the white matter (Fig. 3). The regions in the pyramidal tracts included: the cerebral peduncle, posterior limb of the internal capsule, corona radiata, and centrum semiovale. In the frontobasal area, these included the uncinate fasciculus and forceps minor, while, in the corpus callosum, these included the genu and splenium. One region—the thalamus—was in the gray matter. The FA, ADC, AD, and RD values were calculated for each region. The left and right hemispheres were measured separately for seven regions. Moreover, the ROIs for the genu and splenium of the corpus callosum were drawn in the center of the axial image with one ROI per region.

Statistical Analyses

The statistical analyses were performed using the SPSS software package (IBM SPSS Statistics version 22, Chicago, IL). Means and standard deviations were calculated for each region and parameter, and asymmetries between hemispheres were evaluated using a paired samples t-test. The statistical significance was set to $p < 0.007$, with a Bonferroni correction for seven regions, according to the regions measured in each hemisphere of the brain. The normality of distributions was tested using the Shapiro-Wilk test ($n < 50$). The differences among all the age group means were analyzed using an analysis of variance (ANOVA) for the normally distributed data and Welch's test in inhomogeneous cases, where the variance of the variable differed between the age groups. The Kruskal-Wallis test was used for non-normally distributed data. Correlation analysis between FA, ADC and age from the same data have been published in our previous study (41). In that study, we mostly used a small circle ROI, including a freehand ROI in three regions for better repeatability.

The samples that showed statistically significant differences among the age groups were analyzed by a group comparison between the different age groups. The independent-samples t-test was used with the

normally distributed samples, and the Mann-Whitney U test with the non-normal distributions.

To show the relative variability of each measurement, the percent coefficients of variation (CV%) were calculated according the following equation (with SD = standard deviation and M = mean): (SD/M) x 100% (44). The variability was considered acceptable when the CV% was less than 10% (45). The results between 11 and 20% were considered to be moderate but still adequate. CV% values over 21% were considered too high and inadequate.

The Bland-Altman plots were used as graphical representations for intra- and inter-observer repeatability (44). The 95% limits of agreement and ± 2 standard deviation of the differences were calculated. The better the consistency between the first and repeated measurements, the smaller the difference between the two limits. The intra-observer repeatability (n = 40) was also assessed using intra-class correlation coefficients (ICCs) with an absolute agreement. Two-way mixed option was chosen as the model because the aim was to investigate the repeatability of this specific observer. In this study, the average ICC refers to the repeatability (test-retest) when the same region is measured twice and the final score is the average of two measurements. The single ICC approximates a situation where the measurement would only be made once, as is usually the case in clinical situations. The ICC values were considered to indicate excellent agreement if they were greater than 0.8. ICC results between 0.70 and 0.79 were considered adequate (45), and values below 0.69 were considered inadequate for clinical work. The statistical significance was set to $p < 0.006$, with a Bonferroni correction for nine regions. The calculated inter-observer ICC values were omitted from the results because the number of subjects was too low in the inter-observer measurements.

Results

The data quality was excellent in most cases. In some of the cases, artifacts were detected in the cerebral peduncle, corona radiata, and centrum semiovale (Table 1 and Fig. 2). Significant eddy current artefacts did not occur.

The mean SNR values (± SD) for all regions was 27.7 ± 4.2: the pyramidal tract 30.5 ± 4.2, frontobasal area 24.1 ± 4.7, corpus callosum 25.4 ± 0.3, and thalamus 28.0 ± 4.2.

Mean values

In the Shapiro-Wilks test, 90% of the means were normally distributed ($p < 0.05$). The intra-observer mean values for the FA, ADC, AD, and RD of the sample (n = 40) are shown in Table 2.

In white matter ROIs, the mean FA value was 0.67. The lowest value was found in the corona radiata (0.50), and highest in the genu of the corpus callosum (0.86). The mean ADC value was 0.74×10^{-3} mm^2/s, with lowest value being found in the corona radiata (0.70×10^{-3} mm^2/s) and the highest in the uncinate fasciculus (0.78×10^{-3} mm^2/s). The mean AD value was 1.44×10^{-3} mm^2/s, with the lowest value being found in the corona radiata (1.10×10^{-3} mm^2/s), and highest in the genu of the corpus

callosum (1.82 x 10^{-3} mm^2/s). The mean RD value was 0.39 x 10^{-3} mm^2/s, with the lowest value being found in the genu of the corpus callosum (0.26 x 10^{-3} mm^2/s) and the highest in the forceps minor (0.53 x 10^{-3} mm^2/s). In the gray matter—the thalamus—the corresponding mean values were 0.32 for the FA, 0.76 x 10^{-3} mm^2/s for the ADC, 1.00 x 10^{-3} mm^2/s for AD, and 0.64 x 10^{-3} mm^2/s for RD.

Statistically significant differences between the right and left hemispheres (paired t test, $p < 0.007$) are expressed in Table 2, and the absolute mean values can be found in the table footnotes. In the pyramidal tract, more precisely in the posterior limb of the internal capsule and corona radiata, the FA values were significantly higher and RD values lower in the left hemisphere. The ADC values were lower in the left hemisphere in all four regions of the pyramidal tract. In the cerebral peduncle, the AD value was also lower in the left hemisphere. In both frontobasal regions, the FA values were significantly higher in the right hemisphere.

Significant differences between age groups were found in the frontobasal regions. The FA and AD values were significantly higher and the RD values significantly lower in the youngest age group (18–30 years) compared to the other age groups (31–40, 41–50 and 51–60 years). Specifically, the FA and RD differences were found in both hemispheres and AD differences in the left. For the ADC, there were no significant differences between the groups. The inter-observer mean values were estimated for 15 subjects, and the values are shown in Table 3.

Variation

The intra-observer variations (CV%) are shown in Table 2 (n = 40). In the pyramidal tract, the variation for the FA measurements was 8%. The lowest variation was in the posterior limb of the capsula interna (5%), and the highest in the centrum semiovale (12%). The variation was 11% in the frontobasal area and 5% in the corpus callosum. In the gray matter (thalamus), the variation for the FA was 8%. For the ADC and AD, it was between 3 to 8% with all white matter and gray matter regions. For the RD measurements, the variation in the pyramidal tract was 12%. The lowest variation was in the posterior limb of the capsula interna (8%) and the highest in the cerebral peduncle (18%). The RD variation was 9% in the frontobasal area and 26% in the corpus callosum. In the gray matter (thalamus), the variation was 5%. The inter-observer variation results (CV%) are shown in Table 3.

Reliability

The intra-observer results of the limits of agreement are shown in Table 2. In the white matter, the best intra-observer agreement was found in the posterior limb of the capsula interna with all diffusion parameters. For the ADC, good agreement was also found in the corona radiata, centrum semiovale, uncinate fasciculus, and forceps minor. The largest range between the limits was found in the centrum semiovale for the FA and in the cerebral peduncle for the ADC, AD and RD measurements. The smallest and largest ranges between the 95% limits of agreement for each DTI parameter are presented in the Bland-Altman plots (Figs. 4–5). For the gray matter, the agreement was very good with all DTI parameters (Fig. 6). On average, the 2 SD of the limit of agreement for the intra-observer results was 0.06. The inter-

observer limits of agreement are shown in Table 3, and the smallest ranges between limits are presented in the Bland-Altman plots for each DTI parameter (Fig. 7). In the white matter, the best agreement was found in the posterior limb of the capsula interna with the FA and RD parameters as well as in the centrum semiovale with the ADC and in the corona radiata with AD. On average, the 2 SD of the limit of agreement for the inter-observer results was 0.16.

The intra-observer repeatability results (ICC) are shown in Table 2. For the FA, the mean was 0.87 for the average ICC and 0.78 for the single ICC. The highest average ICC was found in the uncinate fasciculus (0.95), and lowest in the cerebral peduncle (0.75). The average ICC results for the FA were above 0.8, and the single ICCs were above 0.7 in eight of the nine regions. The only area the cerebral peduncle, had coefficients below these results (average 0.75 and single 0.60). For the ADC, the mean value for the average ICC was 0.91 and 0.85 for the single ICC. The highest ICC values were found in the centrum semiovale at both the average (0.98) and single (0.95). The lowest ICC was observed in the cerebral peduncle for both the average (0.80) and single (0.67). For AD, the mean average ICC result was 0.87, and the single ICC result was 0.78. The highest ICC values of AD were found in the splenium of the corpus callosum for both the average (0.94) and single (0.89). The lowest result of AD was in the centrum semiovale at the average (0.76) and single (0.62). For RD, the ICCs results were 0.90 for the average and 0.82 for the single measurement. The best repeatability values of ICCs for the average (0.96) and single (0.93) measurements were both found in the frontobasal area in the uncinate fasciculus. For RD, the lowest value was found in the cerebral peduncle by both the average result (0.76) and the single measurement (0.61).

Discussion

We investigated the intra-and inter-observer reliability and variation of the freehand ROI method in nine different regions of the brain in a sample of 40 healthy adults.

The SNR measurements showed that the image quality was sufficient for reliable quantitative measurements. In general, the SNR of b = 0 s/mm^2 should be at least 20 in order to derive reliable FA values (36). In our study, the SNR was well above 20 in all regions, and the measured SNR values were comparable to other studies (46, 47).

A limitation of this study was that the commercial program did not include eddy current and subject motion corrections. In addition, the spatial resolution was also a bit lower in comparison to that of modern imaging.

FA values are considered to reflect the integrity of the white matter. Although not in itself a specific parameters in a diagnostic sense, it provides indirect information about myelination, fiber packing density, and fiber orientation (48). It is well-known that FA values vary widely at different anatomic levels of the brain (12, 13, 40, 45, 49). Specifically, Lee et al (2009) reported that regional FA values varied from 0.21 in deep gray matter (putamen) to 0.81 in tightly packed parallel white matter tract bundles, such as

the genu of the corpus callosum (12). The corresponding results in this study were 0.32 for deep gray matter (thalamus) and 0.86 for the genu of the corpus callosum. Regions with coherently oriented fibers, such as the cerebral peduncle, internal capsule, and corpus callosum exhibited higher anisotropy than regions with less coherence, such as the centrum semiovale and other subcortical regions (50). Because the regional variability of the FA is in general very large, the possible anatomical mismatch should be taken into account in inter-observer and intergroup comparisons (49). Moreover, less regional variation is found in ADC values (13). In our study, the ADC mean values varied between 0.7–0.8 x 10^{-3} mm^2/s, and in other similar studies the variation was 0.7 to 0.9 x 10^{-3} mm^2/s (45, 51–53). In the frontobasal area, the FA and AD values were lower and the ADC and RD values were higher when compared to other WM regions. The FA values were in line with a tractography study by Deng et al (2018), with a mean FA value of 0.41 (profile 0.3 to 0.52) in the uncinate fasciculus and 0.54 (profile 0.40 to 0.68) in the forceps minor (54). In our study, the FA values were 0.57 and 0.51, respectively. The results of Lieberman et al (2014) were also very close to ours in the uncinate fasciculus (55). The FA and ADC values were almost identical to those found in our previous study (30 subjects) in most of the regions (40). The biggest difference between our present and previous study was found in the genu of the corpus callosum (14%). In this region, measurements were previously made on sagittal images (40) instead of axial images, like in the present study.

Asymmetry between the hemispheres was found in some of the regions. In the pyramidal tracts, such as the posterior limb of the capsula interna and corona radiata, the FA values were higher and the ADC and RD values lower in the left hemisphere. The present results are well in agreement with previous studies (13, 40, 56). Some of the observed asymmetry in our study may be attributed to handedness of the volunteers, because 39 of the 40 volunteers in our study were right-handed. Corresponding hemispheric differences were obtained for right-handers in another study (56). In the case of the corona radiata, the phase artifact could also be one possible explanation. In this region, phase artifacts were present in 55% of cases in the left hemisphere but were not present at all in the right hemisphere. The fat-miss registration just raises the FA value locally and decreases the ADC value. An artifact can affect the ROI in the vicinity, even if the visible part of the artifact is cropped out. In the frontobasal regions, the FA values were found to be higher in the right hemisphere, which is in agreement with previous findings (40, 57). Jahanshad et al (2010) found that the frontal lobe variance in asymmetry is strongly due to genetic factors (57). In our study, higher FA values were usually found in the right hemisphere in the frontobasal area. Bonekamp et al (2007) reported that small hemispheric differences could be due to slight slice angulation (58). Therefore, keeping the same slice position and orientation in longitudinal studies is essential (49).

In terms of age-related changes, we found significant differences between the youngest age group (18–30 years) and other age groups (31–40, 41–50, and 51–60 years). Specifically, in the youngest age group, the FA values were higher and the RD values lower in the frontobasal area in both hemispheres when compared to the other age groups. For FA, this result has already been published in our previous study (41). Other studies have also found changes in the frontal regions of the brain caused by aging (16,

17). In general, several studies have found a negative correlation between age and FA and a positive correlation between age and RD in white matter (21, 22, 59). These variations may be related to changes in myelinization and axon density (17, 60).

In the present study, the acceptable intra-observer variability (≤ 10%) was found in six out of nine regions for FA, while three regions had moderate but adequate variation. For ADC and AD, all regions had acceptable variability. In the RD results, seven out of nine regions had an acceptable or moderate variation and two had high variation (genu and splenium of the corpus callosum). The percent variation of the RD values in the corpus callosum is naturally high, because the mean value is clearly lower than in the other regions. Low RD values are due to the fact that the fibers are tightly packed and parallel to each other. In this case, the variation was not a good indicator for assessing reliability. Overall, the variation results were in line with our previous study (40). It is noteworthy that the freehand method gives an average of 4% lower variations in the pyramidal regions compared to the circle method (13, 41). In contrast, in our study, the freehand method gave a slightly higher variation in the corpus callosum than the circle method in previous studies (13, 41). This may also be due to the fact that in our study, ROIs were plotted on the axial image, whereas in previous studies they were plotted on the sagittal image (13, 41). Thus, in this particular region, it would be better to use the circle method for a sagittal image than the freehand method for an axial image. The inter-observer (n = 15) variability was acceptable or moderate in seven out of nine regions. The inter-observer variabilities are in line with our previous study (40).

Intra-observer repeatability was at a very good level according to the 95% limits of agreement. The results varied according to region, and, with tightly packed white matter tracts, such as the posterior limb of the capsula interna, the difference between the limits was small. Additionally, this difference was greater in areas containing crossing fibers, such as the corona radiata and centrum semiovale. Overall, the results were consistent with our previous research (40). The inter-observer agreement was lower than the intra-observer agreement in all regions, and others have reported similar results (13, 40, 61, 62). It is common for that inter-observer agreement results have been one-third lower than intra-observer results (61, 62).

The intra-observer reliability was high according to the average measures of the ICC analysis. Overall, the average ICC results were excellent for all four parameters. The repeatability result was also excellent (above 0.8) in eight out of nine regions for FA and all regions for the ADC. The repeatability of the freehand method was significantly improved compared to our previous study (40). The average ICC increase was 0.4 (37%) in terms of the FA and ADC parameters. The higher ICC values were probably due to increased observer experience in selecting a slide, avoiding artifacts and the partial volume effect of border areas. The single intra-observer ICC analysis was, on average, excellent in terms of the ADC and RD parameters and moderate in terms of the FA and AD parameters. The results showed excellent or moderate repeatability in seven out of nine regions for all DTI parameters. The region with the highest single ICC values was the forceps minor, with excellent reliability for each parameter. Good reliability was also found in the following regions: the uncinate fasciculus, thalamus, and the genu and splenium of the corpus callosum. High reliability in the corpus callosum is consistent with previous studies with the ROI method (45, 63, 64) but also with the TBSS method (38). Inadequate results (ICC < 0.69) were found in the

cerebral peduncle (FA, ADC and RD) and centrum semiovale (AD). The reason for the inferior reliability of the cerebral peduncle was the susceptibility artifact, more specifically the air-cavity. This artifact causes local changes in the results of the parameters. Although efforts were made to avoid distracted areas in the ROI, the effects of the artifact were also reflected in the surrounding areas. The reason for the low reliability of the centrum semiovale in the AD values can be explained by the multitude of crossing fibers in the subcortical white matter.

Generally, the regions with high reliability and low variation possess some common features. These regions have low anatomical variation and tightly packed fibers with a common orientation (65). These areas also often have a better SNR, fewer partial volume effects, and are also less affected by “crossing” fibers. In addition, the larger ROI size increases the SNR value and improves the repeatability (65). When a larger ROI size is used in a limited region, it is likely that there are more percentages of the same voxels between the two measurements than for a smaller ROI. The results of the repeat measurements are thus close to each other.

In the future studies, larger samples of carefully collected high-spatial and -angular resolution DTI normal data should be required. In those studies, more subjects should be recruited for each age group in order to perform a reliable analysis of the effect of age. In addition, it would be interesting to study how much the reliability of the measurements improve when different methods, such as the ROI, tractography, and TBSS, are used simultaneously.

Conclusions

According to our results, the intra-observer repeatability of the quantitative freehand ROI method can be considered at least adequate. The quantitative freehand ROI method can be considered highly reliable for the average ICC and mostly adequate for the single ICC. The reliability of the single measurements was excellent or moderate in 80% of the regions, including all DTI parameters. In the comparison of parameters, for the single ICCs, most of the repeatability results were excellent in terms of the ADC and RD while only moderate in terms of the FA and AD parameters.

The freehand method is suitable for research work with a well-experienced observer. Measurements should be performed at least twice in the same region to ensure that the results are sufficiently reliable. In only one region—the forceps minor—the single measurement repeatability was excellent for all parameters.

In our study, reliability was undermined by artifacts in some regions such as the cerebral peduncle, corona radiata and centrum semiovale.

When using the results of healthy adults as a control for patient groups, it should be noted that the results are most reliable on adults less than 30 years of age whose brain white matter does not yet have age-related changes.

Declarations

Ethics approval and consent to participate

An ethics approval was obtained from the Ethical Committee of the Pirkanmaa Hospital District. Informed consent was obtained from all participants. All methods were carried out in accordance with relevant guidelines and regulations.

Consent for publication

Not applicable.

Availability of data and materials

The datasets used and/or analysed during the current study are available from the corresponding author on reasonable request.

Competing interests

The authors have no competing interests.

Funding

This study was financially partly supported by Tampere University Hospital Support Foundation, Tampere University Hospital. The funding organization had no role in the design, implementation, and manuscript of the study.

Authors' contributions

J.Ö. and T.L. contributed to the design of the study. T.L. recruits control subjects. U.H. designed and performed the measurements, analyzed the results, made plots and figures and wrote the manuscript as a first-author. A.B. performed inter-observer measurements and actively participated in the manuscript writing process. H.E acted as supervisor in the manuscript and technical section. M.H. contributes to statistical analyzes. T.I. critically reviewed the analyzes and commented on the manuscript. Everyone participated in the evaluation of the manuscript.

Acknowledgements

Not applicable.

Authors' information

Ullamari Hakulinen ullamari.hakulinen@pshp.fi

Antti Brander antti.brander@pp.fimnet.fi

Tero Ilvesmäki tero.ilvesmaki@satshp.fi

Mika Helminen mika.helminen@tuni.fi

Juha Öhman juha.ohman@pshp.fi

Teemu Luoto teemu.luoto@pshp.fi

Hannu Eskola hannu.eskola@tuni.fi

Acknowledgements

Thanks to my colleague Pertti Ryymin, who checked the technical MRI section of the background.

Funding

This study was financially partly supported by Tampere University Hospital Support Foundation, Tampere University Hospital. The funding organization had no role in the design, implementation, and manuscript of the study.

References

1. Mori S, Crain BJ, Chacko VP, van Zijl PC. Three-dimensional tracking of axonal projections in the brain by magnetic resonance imaging. Ann Neurol. 1999 Feb;45(2):265-9. doi: 10.1002/1531-8249(199902)45:2<265::aid-ana21>3.0.co;2-3. PMID: 9989633.
2. Assaf Y, Pasternak O. Diffusion tensor imaging (DTI)-based white matter mapping in brain research: a review. J Mol Neurosci. 2008;34(1):51–61. doi: 10.1007/s12031-007-0029-0. PMID: 18157658.
3. Farrell JA, Landman BA, Jones CK, Smith SA, Prince JL, van Zijl PC, Mori S. Effects of signal-to-noise ratio on the accuracy and reproducibility of diffusion tensor imaging-derived fractional anisotropy, mean diffusivity, and principal eigenvector measurements at 1.5 T. J Magn Reson Imaging. 2007 Sep;26(3):756–67. doi: 10.1002/jmri.21053. PMID: 17729339; PMCID: PMC2862967.
4. Budde MD, Xie M, Cross AH, Song SK. Axial diffusivity is the primary correlate of axonal injury in the experimental autoimmune encephalomyelitis spinal cord: a quantitative pixelwise analysis. J Neurosci. 2009 Mar 4;29(9):2805-13. doi: 10.1523/JNEUROSCI.4605-08.2009. PMID: 19261876; PMCID: PMC2673458.
5. Song SK, Yoshino J, Le TQ, Lin SJ, Sun SW, Cross AH, Armstrong RC. Demyelination increases radial diffusivity in corpus callosum of mouse brain. Neuroimage. 2005 May 15;26(1):132 – 40. doi: 10.1016/j.neuroimage.2005.01.028. PMID: 15862213.
6. Alexander AL, Lee JE, Lazar M, Field AS. Diffusion tensor imaging of the brain. Neurotherapeutics. 2007 Jul;4(3):316–29. doi: 10.1016/j.nurt.2007.05.011. PMID: 17599699; PMCID: PMC2041910.
7. Song SK, Sun SW, Ramsbottom MJ, Chang C, Russell J, Cross AH. Dysmyelination revealed through MRI as increased radial (but unchanged axial) diffusion of water. Neuroimage. 2002 Nov;17(3):1429-

36. doi: 10.1006/nimg.2002.1267. PMID: 12414282.

8. Perlbarg V, Puybasset L, Tollard E, Lehéricy S, Benali H, Galanaud D. Relation between brain lesion location and clinical outcome in patients with severe traumatic brain injury: a diffusion tensor imaging study using voxel-based approaches. Hum Brain Mapp. 2009 Dec;30(12):3924–33. doi: 10.1002/hbm.20817. PMID: 19507154; PMCID: PMC6870894.
9. Boespflug EL, Storrs JM, Allendorfer JB, Lamy M, Eliassen JC, Page S. Mean diffusivity as a potential diffusion tensor biomarker of motor rehabilitation after electrical stimulation incorporating task specific exercise in stroke: a pilot study. Brain Imaging Behav. 2014 Sep;8(3):359 – 69. doi: 10.1007/s11682-011-9144-1. PMID: 22203524.
10. Klawiter EC, Schmidt RE, Trinkaus K, Liang HF, Budde MD, Naismith RT, Song SK, Cross AH, Benzinger TL. Radial diffusivity predicts demyelination in ex vivo multiple sclerosis spinal cords. Neuroimage. 2011 Apr 15;55(4):1454-60. doi: 10.1016/j.neuroimage.2011.01.007. Epub 2011 Jan 13. PMID: 21238597; PMCID: PMC3062747.
11. Mukherjee P. Diffusion tensor imaging and fiber tractography in acute stroke. Neuroimaging Clin N Am. 2005 Aug;15(3):655 – 65, xii. doi: 10.1016/j.nic.2005.08.010. PMID: 16360595.
12. Lee CE, Danielian LE, Thomasson D, Baker EH. Normal regional fractional anisotropy and apparent diffusion coefficient of the brain measured on a 3 T MR scanner. Neuroradiology. 2009 Jan;51(1):3–9. doi: 10.1007/s00234-008-0441-3. Epub 2008 Aug 13. PMID: 18704391.
13. Brander A, Kataja A, Saastamoinen A, Ryymin P, Huhtala H, Ohman J, Soimakallio S, Dastidar P. Diffusion tensor imaging of the brain in a healthy adult population: Normative values and measurement reproducibility at 3 T and 1.5 T. Acta Radiol. 2010 Sep;51(7):800-7. doi: 10.3109/02841851.2010.495351. PMID: 20707664.
14. Ilvesmäki T, Luoto TM, Hakulinen U, Brander A, Ryymin P, Eskola H, Iverson GL, Ohman J. Acute mild traumatic brain injury is not associated with white matter change on diffusion tensor imaging. Brain. 2014 Jul;137(Pt 7):1876-82. doi: 10.1093/brain/awu095. Epub 2014 May 11. PMID: 24818956.
15. Sala S, Agosta F, Pagani E, Copetti M, Comi G, Filippi M. Microstructural changes and atrophy in brain white matter tracts with aging. Neurobiol Aging. 2012 Mar;33(3):488–498.e2. doi: 10.1016/j.neurobiolaging.2010.04.027. Epub 2010 Jul 1. PMID: 20594616.
16. Yoon B, Shim YS, Lee KS, Shon YM, Yang DW. Region-specific changes of cerebral white matter during normal aging: a diffusion-tensor analysis. Arch Gerontol Geriatr. 2008 Jul-Aug;47(1):129–38. doi: 10.1016/j.archger.2007.07.004. Epub 2007 Aug 30. PMID: 17764763.
17. Bach M, Laun FB, Leemans A, Tax CM, Biessels GJ, Stieltjes B, Maier-Hein KH. Methodological considerations on tract-based spatial statistics (TBSS). Neuroimage. 2014 Oct 15;100:358–69. doi: 10.1016/j.neuroimage.2014.06.021. Epub 2014 Jun 16. PMID: 24945661.
18. Ilvesmäki T, Koskinen E, Brander A, Luoto T, Öhman J, Eskola H. Spinal cord injury induces widespread chronic changes in cerebral white matter. Hum Brain Mapp. 2017 Jul;38(7):3637–3647. doi: 10.1002/hbm.23619. Epub 2017 Apr 21. PMID: 28429407; PMCID: PMC6866745.

19. Choi JY, Hart T, Whyte J, Rabinowitz AR, Oh SH, Lee J, Kim JJ. Myelin water imaging of moderate to severe diffuse traumatic brain injury. Neuroimage Clin. 2019;22:101785. doi: 10.1016/j.nicl.2019.101785. Epub 2019 Mar 16. PMID: 30927603; PMCID: PMC6444291.
20. Dailey NS, Smith R, Bajaj S, Alkozei A, Gottschlich MK, Raikes AC, Satterfield BC, Killgore WDS. Elevated Aggression and Reduced White Matter Integrity in Mild Traumatic Brain Injury: A DTI Study. Front Behav Neurosci. 2018 Jun 27;12:118. doi: 10.3389/fnbeh.2018.00118. PMID: 30013466; PMCID: PMC6036267.
21. Cox SR, Ritchie SJ, Tucker-Drob EM, Liewald DC, Hagenaars SP, Davies G, Wardlaw JM, Gale CR, Bastin ME, Deary IJ. Ageing and brain white matter structure in 3,513 UK Biobank participants. Nat Commun. 2016 Dec 15;7:13629. doi: 10.1038/ncomms13629. PMID: 27976682; PMCID: PMC5172385.
22. Kodiweera C, Alexander AL, Harezlak J, McAllister TW, Wu YC. Age effects and sex differences in human brain white matter of young to middle-aged adults: A DTI, NODDI, and q-space study. Neuroimage. 2016 Mar;128:180–192. doi: 10.1016/j.neuroimage.2015.12.033. Epub 2015 Dec 24. PMID: 26724777; PMCID: PMC4824064.
23. Banaszek A, Bladowska J, Pokryszko-Dragan A, Podemski R, Sąsiadek MJ. Evaluation of the Degradation of the Selected Projectile, Commissural and Association White Matter Tracts Within Normal Appearing White Matter in Patients with Multiple Sclerosis Using Diffusion Tensor MR Imaging - a Preliminary Study. Pol J Radiol. 2015 Oct 5;80:457–63. doi: 10.12659/PJR.894661. PMID: 26516389; PMCID: PMC4603607.
24. Lipton ML, Gulko E, Zimmerman ME, Friedman BW, Kim M, Gellella E, Gold T, Shifteh K, Ardekani BA, Branch CA. Diffusion-tensor imaging implicates prefrontal axonal injury in executive function impairment following very mild traumatic brain injury. Radiology. 2009 Sep;252(3):816–24. doi: 10.1148/radiol.2523081584. Epub 2009 Jun 30. PMID: 19567646.
25. Messé A, Caplain S, Pélégrini-Issac M, Blancho S, Montreuil M, Lévy R, Lehéricy S, Benali H. Structural integrity and postconcussion syndrome in mild traumatic brain injury patients. Brain Imaging Behav. 2012 Jun;6(2):283 – 92. doi: 10.1007/s11682-012-9159-2. PMID: 22477019.
26. Shen JM, Xia XW, Kang WG, Yuan JJ, Sheng L. The use of MRI apparent diffusion coefficient (ADC) in monitoring the development of brain infarction. BMC Med Imaging. 2011 Jan 6;11:2. doi: 10.1186/1471-2342-11-2. PMID: 21211049; PMCID: PMC3022840.
27. Alegiani AC, MacLean S, Braass H, Gellißen S, Cho TH, Derex L, Hermier M, Berthezene Y, Nighoghossian N, Gerloff C, Fiehler J, Thomalla G. Dynamics of Water Diffusion Changes in Different Tissue Compartments From Acute to Chronic Stroke-A Serial Diffusion Tensor Imaging Study. Front Neurol. 2019 Feb 26;10:158. doi: 10.3389/fneur.2019.00158. PMID: 30863361; PMCID: PMC6399390.
28. Jones DK. Precision and accuracy in diffusion tensor magnetic resonance imaging. Top Magn Reson Imaging. 2010 Apr;21(2):87–99. doi: 10.1097/RMR.0b013e31821e56ac. PMID: 21613874.

29. Jones DK, Cercignani M. Twenty-five pitfalls in the analysis of diffusion MRI data. NMR Biomed. 2010 Aug;23(7):803 – 20. doi: 10.1002/nbm.1543. PMID: 20886566.
30. Westin CF, Maier SE, Mamata H, Nabavi A, Jolesz FA, Kikinis R. Processing and visualization for diffusion tensor MRI. Med Image Anal. 2002 Jun;6(2):93–108. doi: 10.1016/s1361-8415(02)00053-1. PMID: 12044998.
31. Anderson AW. Theoretical analysis of the effects of noise on diffusion tensor imaging. Magn Reson Med. 2001 Dec;46(6):1174-88. doi: 10.1002/mrm.1315. PMID: 11746585.
32. Lazar M, Alexander AL. An error analysis of white matter tractography methods: synthetic diffusion tensor field simulations. Neuroimage. 2003 Oct;20(2):1140-53. doi: 10.1016/S1053-8119(03)00277-5. PMID: 14568483.
33. Leemans A, Jones DK. The B-matrix must be rotated when correcting for subject motion in DTI data. Magn Reson Med. 2009 Jun;61(6):1336-49. doi: 10.1002/mrm.21890. PMID: 19319973.
34. Dietrich O, Reiser MF, Schoenberg SO. Artifacts in 3-T MRI: physical background and reduction strategies. Eur J Radiol. 2008 Jan;65(1):29–35. doi: 10.1016/j.ejrad.2007.11.005. Epub 2007 Dec 26. PMID: 18162353.
35. Heiervang E, Behrens TE, Mackay CE, Robson MD, Johansen-Berg H. Between session reproducibility and between subject variability of diffusion MR and tractography measures. Neuroimage. 2006 Nov 15;33(3):867–77. doi: 10.1016/j.neuroimage.2006.07.037. Epub 2006 Sep 26. PMID: 17000119.
36. Mukherjee P, Chung SW, Berman JI, Hess CP, Henry RG. Diffusion tensor MR imaging and fiber tractography: technical considerations. AJNR Am J Neuroradiol. 2008 May;29(5):843–52. doi: 10.3174/ajnr.A1052. Epub 2008 Mar 13. PMID: 18339719.
37. Smith SM, Jenkinson M, Johansen-Berg H, Rueckert D, Nichols TE, Mackay CE, Watkins KE, Ciccarelli O, Cader MZ, Matthews PM, Behrens TE. Tract-based spatial statistics: voxelwise analysis of multi-subject diffusion data. Neuroimage. 2006 Jul 15;31(4):1487–505. doi: 10.1016/j.neuroimage.2006.02.024. Epub 2006 Apr 19. PMID: 16624579.
38. Merisaari H, Tuulari JJ, Karlsson L, Scheinin NM, Parkkola R, Saunavaara J, Lähdesmäki T, Lehtola SJ, Keskinen M, Lewis JD, Evans AC, Karlsson H. Test-retest reliability of Diffusion Tensor Imaging metrics in neonates. Neuroimage. 2019 Aug 15;197:598–607. doi: 10.1016/j.neuroimage.2019.04.067. Epub 2019 Apr 25. PMID: 31029873.
39. Lilja Y, Gustafsson O, Ljungberg M, Nilsson D, Starck G. Impact of region-of-interest method on quantitative analysis of DTI data in the optic tracts. BMC Med Imaging. 2016 Jul 11;16(1):42. doi: 10.1186/s12880-016-0145-9. PMID: 27400959; PMCID: PMC4940685.
40. Hakulinen U, Brander A, Ryymin P, Öhman J, Soimakallio S, Helminen M, Dastidar P, Eskola H. Repeatability and variation of region-of-interest methods using quantitative diffusion tensor MR imaging of the brain. BMC Med Imaging. 2012 Oct 11;12:30. doi: 10.1186/1471-2342-12-30. PMID: 23057584; PMCID: PMC3533516.
41. Nenonen M, Hakulinen U, Brander A, Ohman J, Dastidar P, Luoto TM. Possible confounding factors on cerebral diffusion tensor imaging measurements. Acta Radiol Open. 2015 Jan

24;4(2):2047981614546795. doi: 10.1177/2047981614546795. PMID: 25793107; PMCID: PMC4364398.

42. Koskinen E, Brander A, Hakulinen U, Luoto T, Helminen M, Ylinen A, Ohman J. Assessing the state of chronic spinal cord injury using diffusion tensor imaging. J Neurotrauma. 2013 Sep 15;30(18):1587-95. doi: 10.1089/neu.2013.2943. Epub 2013 Aug 9. PMID: 23758292.
43. Wakana S, Jiang H, Nagae-Poetscher LM, van Zijl PC, Mori S. Fiber tract-based atlas of human white matter anatomy. Radiology. 2004 Jan;230(1):77–87. doi: 10.1148/radiol.2301021640. Epub 2003 Nov 26. PMID: 14645885.
44. Bland JM, Altman DG. Statistical methods for assessing agreement between two methods of clinical measurement. Lancet. 1986 Feb 8;1(8476):307 – 10. PMID: 2868172.
45. Marenco S, Rawlings R, Rohde GK, Barnett AS, Honea RA, Pierpaoli C, Weinberger DR. Regional distribution of measurement error in diffusion tensor imaging. Psychiatry Res. 2006 Jun 30;147(1):69–78. doi: 10.1016/j.pscychresns.2006.01.008. Epub 2006 Jun 21. PMID: 16797169; PMCID: PMC1941705.
46. Polders DL, Leemans A, Hendrikse J, Donahue MJ, Luijten PR, Hoogduin JM. Signal to noise ratio and uncertainty in diffusion tensor imaging at 1.5, 3.0, and 7.0 Tesla. J Magn Reson Imaging. 2011 Jun;33(6):1456-63. doi: 10.1002/jmri.22554. PMID: 21591016.
47. Laganà M, Rovaris M, Ceccarelli A, Venturelli C, Marini S, Baselli G. DTI parameter optimisation for acquisition at 1.5T: SNR analysis and clinical application. Comput Intell Neurosci. 2010;2010:254032. doi: 10.1155/2010/254032. Epub 2010 Jan 5. PMID: 20069121; PMCID: PMC2804108.
48. Shimony JS, McKinstry RC, Akbudak E, Aronovitz JA, Snyder AZ, Lori NF, Cull TS, Conturo TE. Quantitative diffusion-tensor anisotropy brain MR imaging: normative human data and anatomic analysis. Radiology. 1999 Sep;212(3):770 – 84. doi: 10.1148/radiology.212.3.r99au51770. PMID: 10478246.
49. Virta A, Barnett A, Pierpaoli C. Visualizing and characterizing white matter fiber structure and architecture in the human pyramidal tract using diffusion tensor MRI. Magn Reson Imaging. 1999 Oct;17(8):1121-33. doi: 10.1016/s0730-725x(99)00048-x. PMID: 10499674.
50. Pierpaoli C, Jezzard P, Basser PJ, Barnett A, Di Chiro G. Diffusion tensor MR imaging of the human brain. Radiology. 1996 Dec;201(3):637 – 48. doi: 10.1148/radiology.201.3.8939209. PMID: 8939209.
51. Bisdas S, Bohning DE, Besenski N, Nicholas JS, Rumboldt Z. Reproducibility, interrater agreement, and age-related changes of fractional anisotropy measures at 3T in healthy subjects: effect of the applied b-value. AJNR Am J Neuroradiol. 2008 Jun;29(6):1128–33. doi: 10.3174/ajnr.A1044. Epub 2008 Mar 27. PMID: 18372415.
52. Huisman TA, Loenneker T, Barta G, Bellemann ME, Hennig J, Fischer JE, Il'yasov KA. Quantitative diffusion tensor MR imaging of the brain: field strength related variance of apparent diffusion coefficient (ADC) and fractional anisotropy (FA) scalars. Eur Radiol. 2006 Aug;16(8):1651-8. doi: 10.1007/s00330-006-0175-8. Epub 2006 Mar 11. PMID: 16532356.

53. Hunsche S, Moseley ME, Stoeter P, Hedehus M. Diffusion-tensor MR imaging at 1.5 and 3.0 T: initial observations. Radiology. 2001 Nov;221(2):550-6. doi: 10.1148/radiol.2212001823. PMID: 11687703
54. Deng F, Zhao L, Liu C, Lu M, Zhang S, Huang H, Chen L, Wu X, Niu C, He Y, Wang J, Huang R. Plasticity in deep and superficial white matter: a DTI study in world class gymnasts. Brain Struct Funct. 2018 May;223(4):1849–1862. doi: 10.1007/s00429-017-1594-9. Epub 2017 Dec 18. PMID: 29250703.
55. Lieberman G, Shpaner M, Watts R, Andrews T, Filippi CG, Davis M, Naylor MR. White matter involvement in chronic musculoskeletal pain. J Pain. 2014 Nov;15(11):1110–1119. doi: 10.1016/j.jpain.2014.08.002. Epub 2014 Aug 15. PMID: 25135468; PMCID: PMC4254784.
56. Seizeur R, Magro E, Prima S, Wiest-Daesslé N, Maumet C, Morandi X. Corticospinal tract asymmetry and handedness in right- and left-handers by diffusion tensor tractography. Surg Radiol Anat. 2014 Mar;36(2):111–24. doi: 10.1007/s00276-013-1156-7. Epub 2013 Jun 27. PMID: 23807198; PMCID: PMC5225265.
57. Jahanshad N, Lee AD, Barysheva M, McMahon KL, de Zubicaray GI, Martin NG, Wright MJ, Toga AW, Thompson PM. Genetic influences on brain asymmetry: a DTI study of 374 twins and siblings. Neuroimage. 2010 Aug 15;52(2):455 – 69. doi: 10.1016/j.neuroimage.2010.04.236. Epub 2010 Apr 27. PMID: 20430102; PMCID: PMC3086641.
58. Bonekamp D, Nagae LM, Degaonkar M, Matson M, Abdalla WM, Barker PB, Mori S, Horská A. Diffusion tensor imaging in children and adolescents: reproducibility, hemispheric, and age-related differences. Neuroimage. 2007 Jan 15;34(2):733 – 42. doi: 10.1016/j.neuroimage.2006.09.020. Epub 2006 Nov 7. PMID: 17092743; PMCID: PMC1815474.
59. Inano S, Takao H, Hayashi N, Abe O, Ohtomo K. Effects of age and gender on white matter integrity. AJNR Am J Neuroradiol. 2011 Dec;32(11):2103–9. doi: 10.3174/ajnr.A2785. Epub 2011 Oct 13. PMID: 21998104.
60. Lebel C, Gee M, Camicioli R, Wieler M, Martin W, Beaulieu C. Diffusion tensor imaging of white matter tract evolution over the lifespan. Neuroimage. 2012 Mar;60(1):340–52. doi: 10.1016/j.neuroimage.2011.11.094. Epub 2011 Dec 8. PMID: 22178809.
61. Ciccarelli O, Parker GJ, Toosy AT, Wheeler-Kingshott CA, Barker GJ, Boulby PA, Miller DH, Thompson AJ. From diffusion tractography to quantitative white matter tract measures: a reproducibility study. Neuroimage. 2003 Feb;18(2):348 – 59. doi: 10.1016/s1053-8119(02)00042-3. PMID: 12595188.
62. Müller MJ, Mazanek M, Weibrich C, Dellani PR, Stoeter P, Fellgiebel A. Distribution characteristics, reproducibility, and precision of region of interest-based hippocampal diffusion tensor imaging measures. AJNR Am J Neuroradiol. 2006 Feb;27(2):440–6. PMID: 16484426.
63. Pfefferbaum A, Adalsteinsson E, Sullivan EV. Replicability of diffusion tensor imaging measurements of fractional anisotropy and trace in brain. J Magn Reson Imaging. 2003 Oct;18(4):427 – 33. doi: 10.1002/jmri.10377. PMID: 14508779.
64. Papinutto ND, Maule F, Jovicich J. Reproducibility and biases in high field brain diffusion MRI: An evaluation of acquisition and analysis variables. Magn Reson Imaging. 2013 Jul;31(6):827–39. doi:

10.1016/j.mri.2013.03.004. Epub 2013 Apr 24. PMID: 23623031.

65. Stieltjes B, Kaufmann WE, van Zijl PC, Fredericksen K, Pearlson GD, Solaiyappan M, Mori S. Diffusion tensor imaging and axonal tracking in the human brainstem. Neuroimage. 2001 Sep;14(3):723 – 35. doi: 10.1006/nimg.2001.0861. PMID: 11506544.

Tables

Due to technical limitations, table 1,2,3 is only available as a download in the Supplemental Files section.

Figures

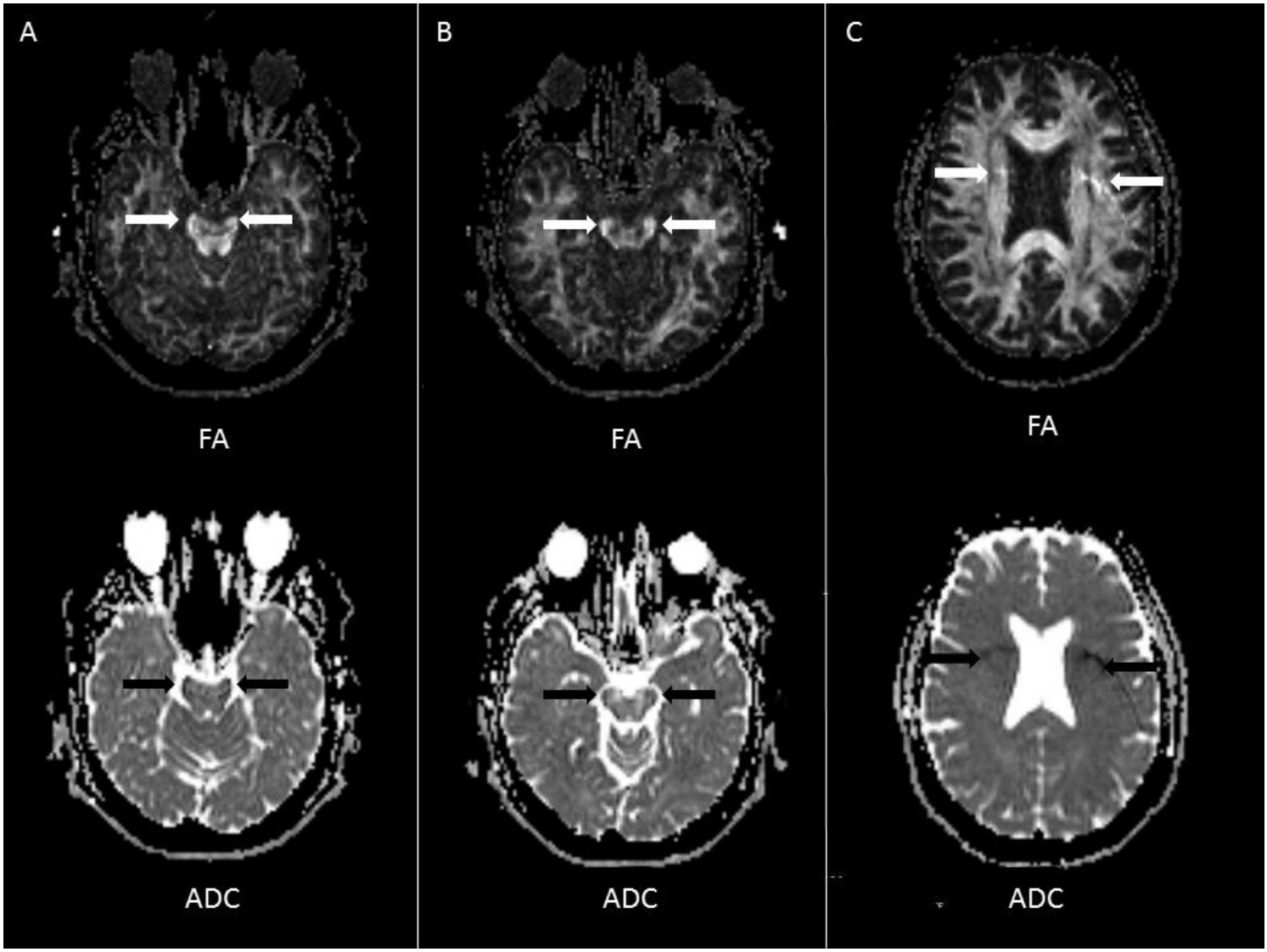

Figure 1

Axial FA and ADC maps with examples of common artifacts: A) distortion in the cerebral peduncle, B) susceptibility artifact (air-cavity) in the cerebral peduncle, and C) phase artifact (fat-miss registration) in the corona radiata.

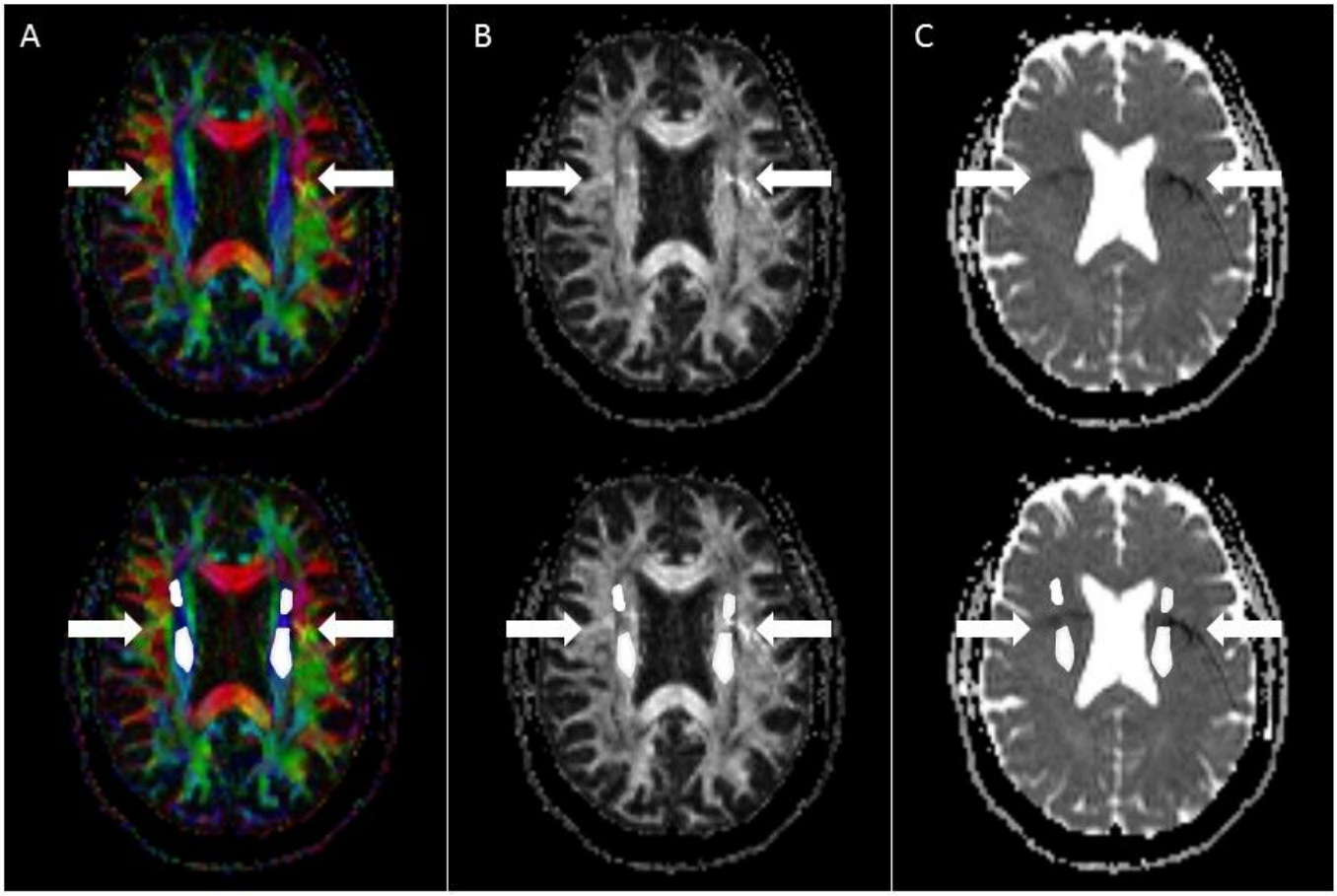

Figure 2

Examples of FA and ADC maps with a phase artifact (fat-miss registration) in the corona radiata and how the artifact was excluded from the ROIs: A) axial FA color map, B) axial FA map, and C) axial ADC map.

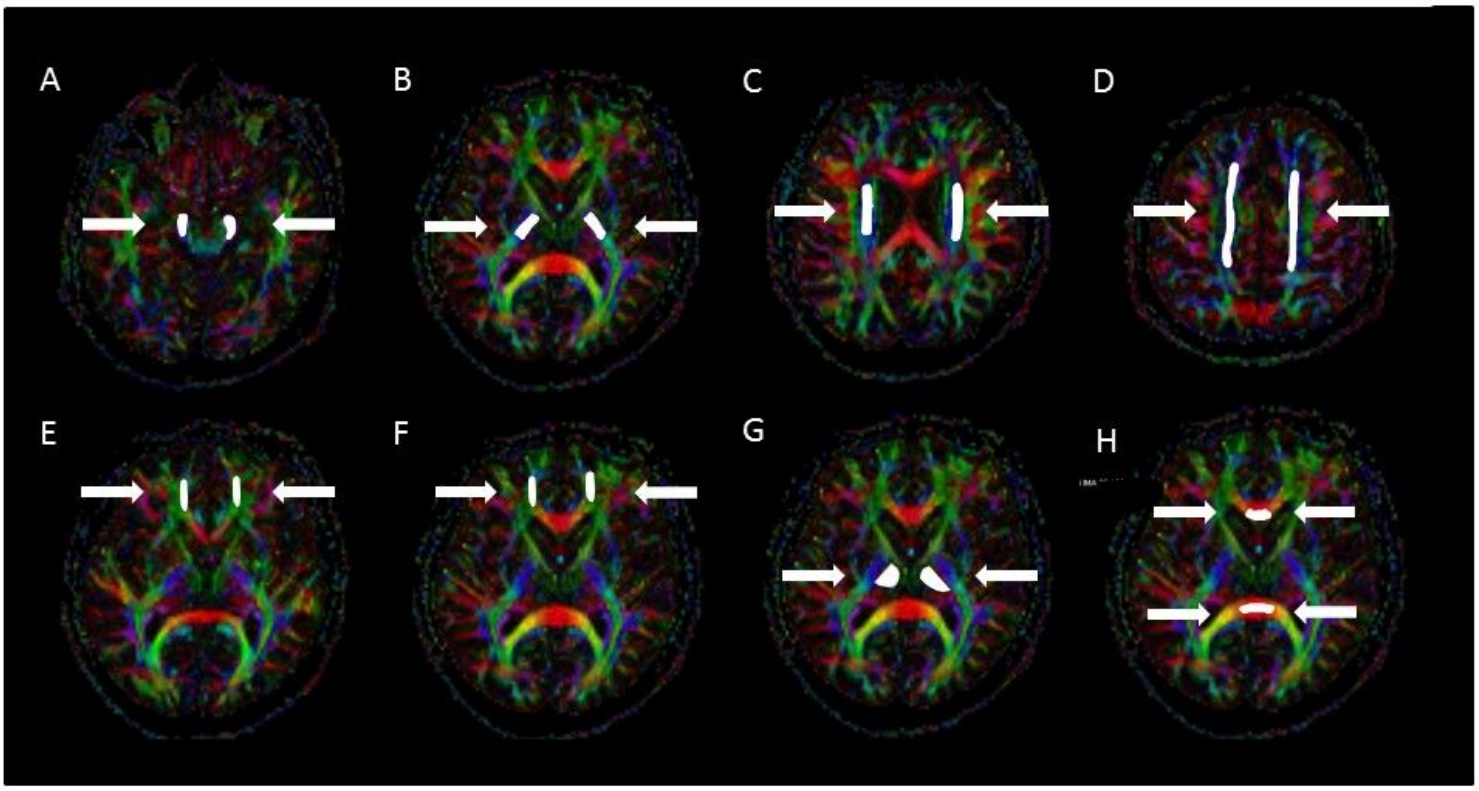

Figure 3

Axial FA color maps with the measured freehand ROIs (regions-of-interest): A) cerebral peduncle, B) posterior limb of the internal capsule, C) corona radiata, D) centrum semiovale, E) uncinate fasciculus F) forceps minor, G) thalamus, and H) genu and splenium of the corpus callosum.

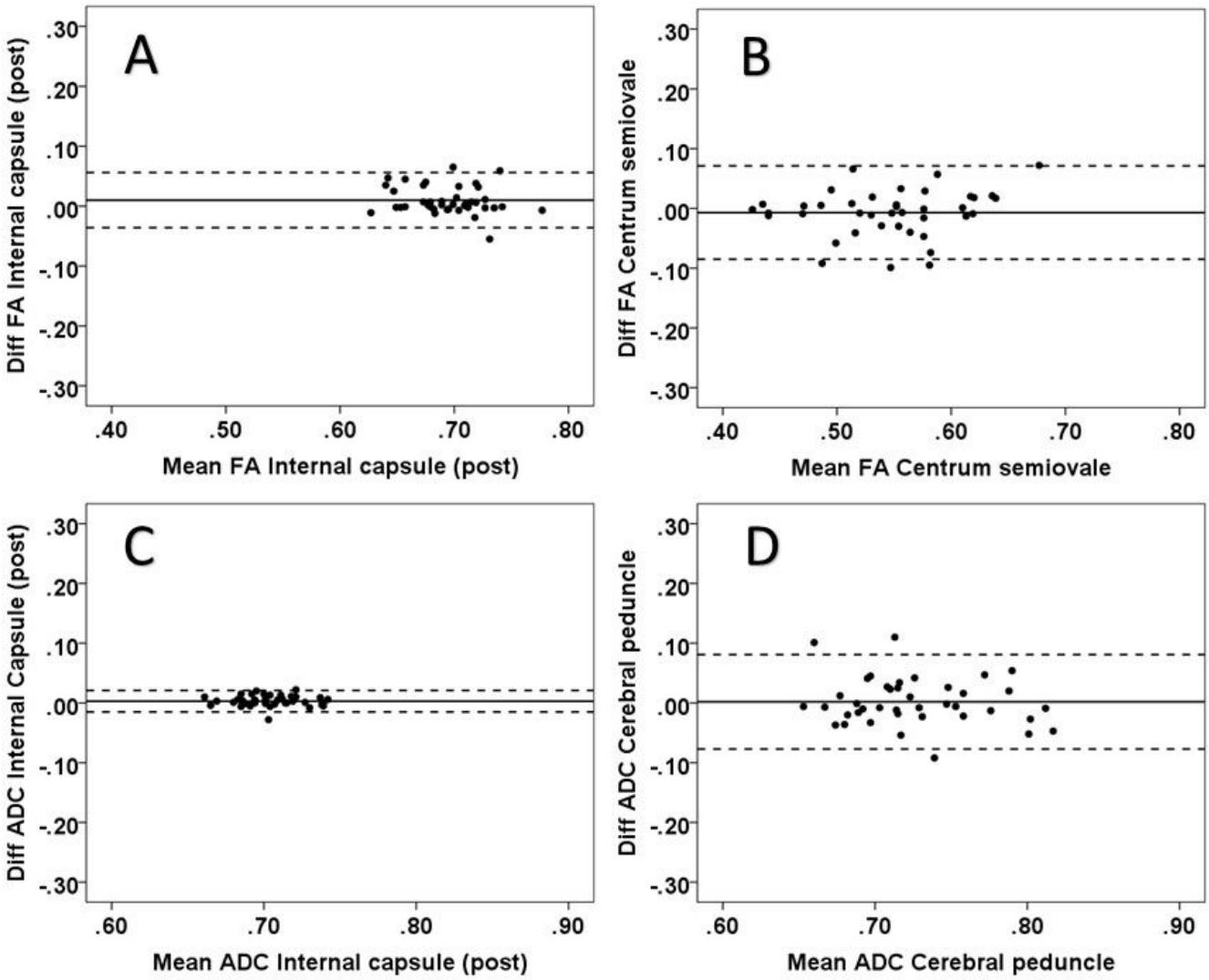

Figure 4

The intra-observer reliability for FA and ADC in select white matter regions; the Bland-Altman plots show minimum and maximum differences with 95% limits of agreement (dotted lines): A) posterior limb of the internal capsule (min FA), B) cerebral peduncle (max FA), C) posterior limb of the internal capsule (min ADC), and D) corona radiata (max ADC).

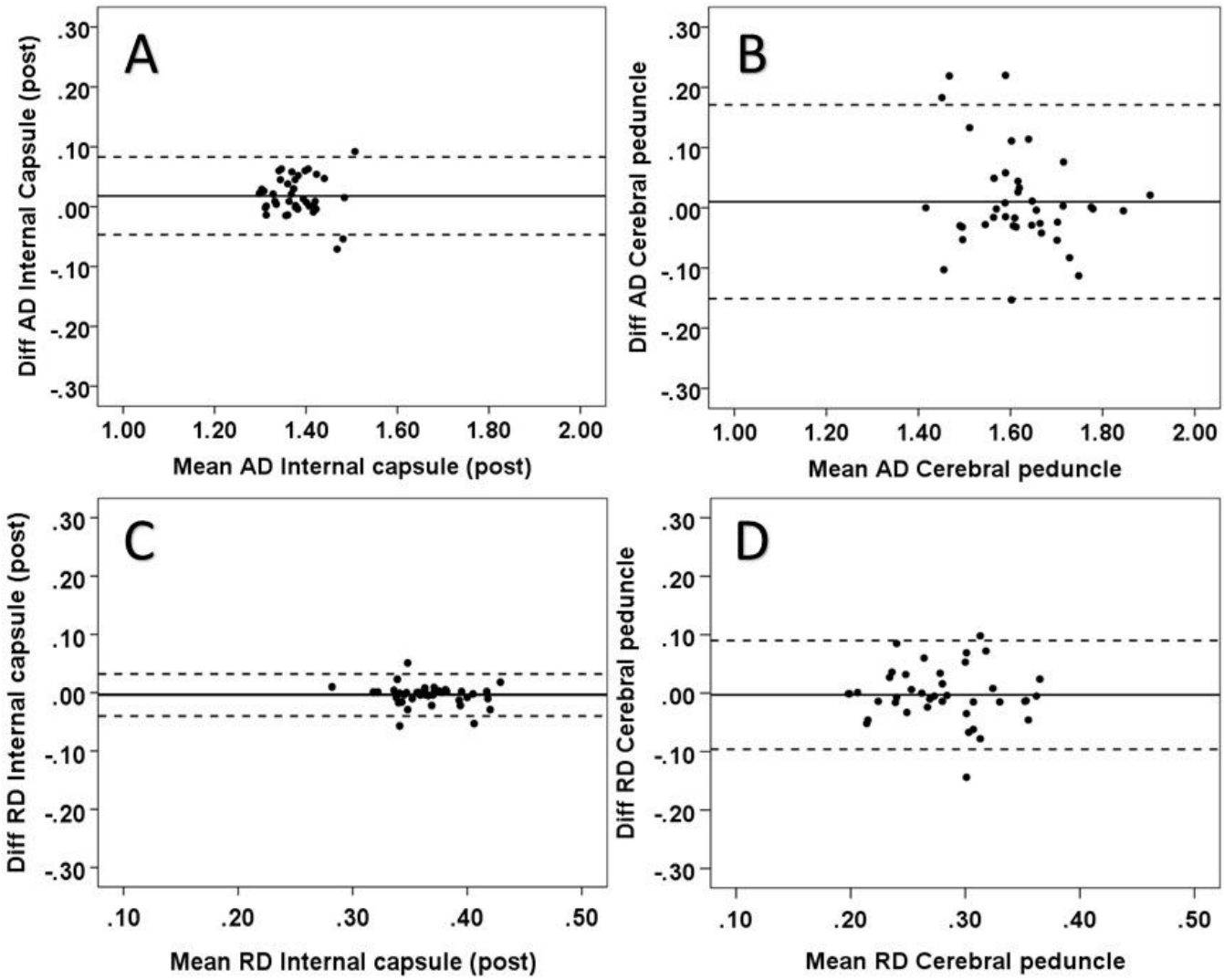

Figure 5

Intra-observer reliability for AD and RD in select white matter regions; the Bland-Altman plots show minimum and maximum differences with 95% limits of agreement (dotted lines): A) posterior limb of the internal capsule (min AD), B) cerebral peduncle (max AD), C) posterior limb of the internal capsule (min RD), and D) corona radiata (max RD).

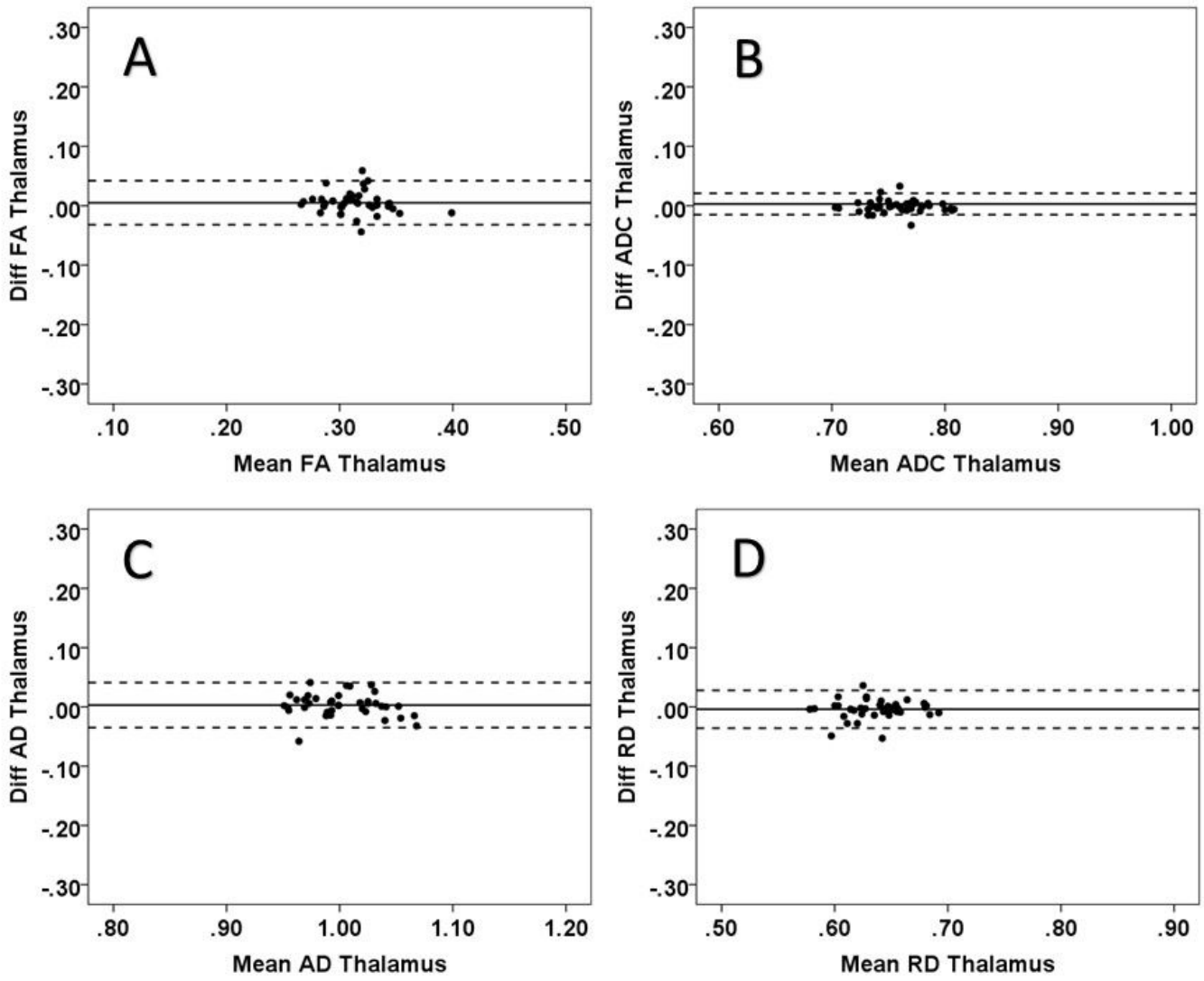

Figure 6

Intra-observer reliability for all parameters in the thalamus; the Bland-Altman plots show 95% limits of agreement (dotted lines): A) thalamus (FA), B) thalamus (ADC), C) thalamus (AD), and D) thalamus (RD).

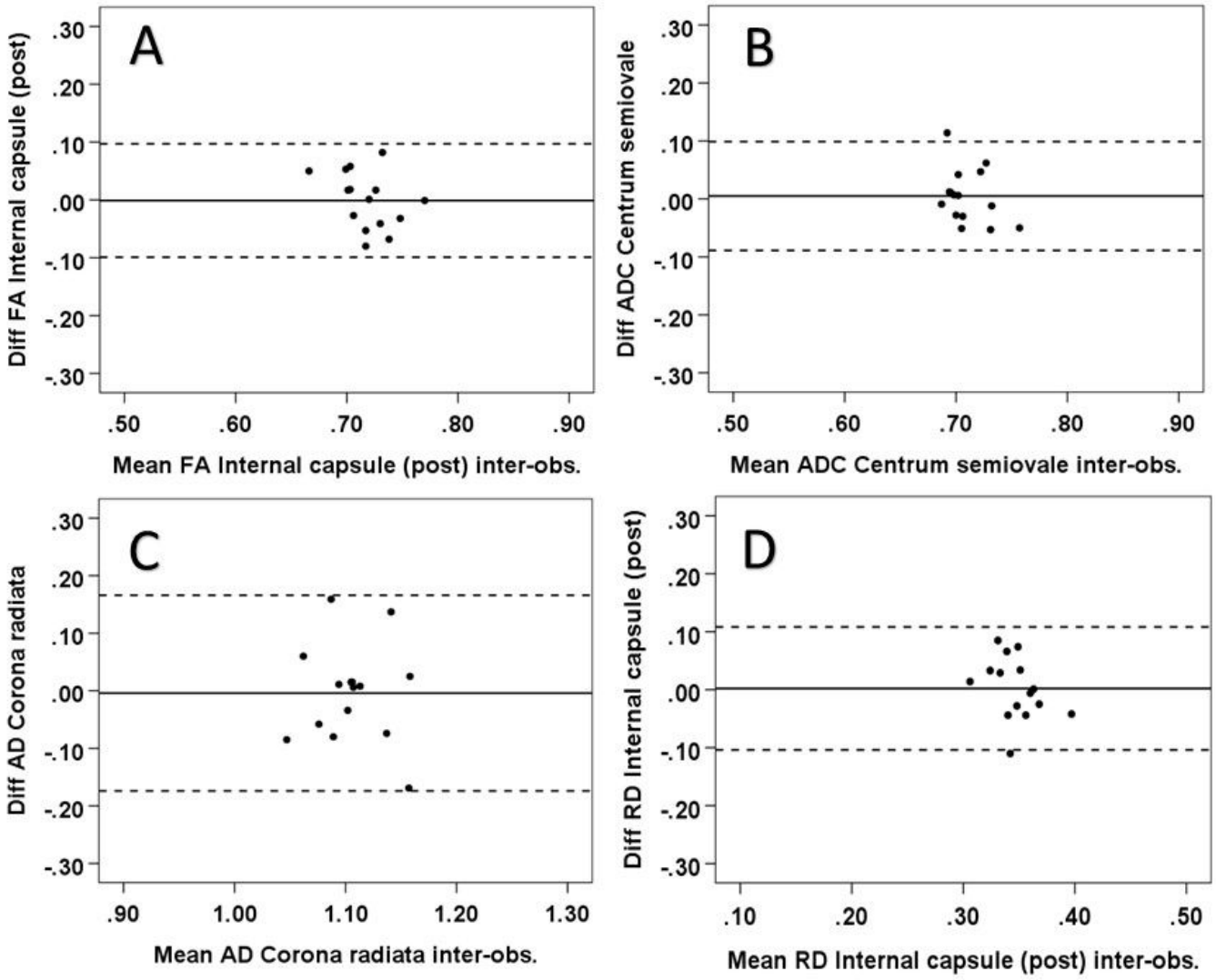

Figure 7

Inter-observer reliability; the Bland-Altman plots show minimum differences with 95% limits of agreement (dotted lines) with all parameters: A) posterior limb of the internal capsule (FA), B) centrum semivale (ADC), C) corona radiata (AD), and D) posterior limb of the internal capsule (RD).

Supplementary Files

This is a list of supplementary files associated with this preprint. Click to download.

- Table1.xlsx
- Table2.xlsx
- Table3.xlsx